Approximate particle number projection for rotating nuclei

P. Magierski and S. Ćwiok

Institute of Physics, Warsaw University of Technology, ul. Koszykowa 75, PL–00-662 Warsaw, Poland

J. Dobaczewski

Institute of Theoretical Physics, Warsaw University, ul. Hoża 69, PL–00-681 Warsaw, Poland

W. Nazarewicz*

*Joint Institute for Heavy-Ion Research, Physics Division, Oak Ridge National Laboratory,
P.O. Box 2008, Oak Ridge, Tennessee 37831
and Department of Physics, University of Tennessee, Knoxville, Tennessee 37996*
(Received 22 April 1993)

Pairing correlations in rotating nuclei are discussed within the Lipkin-Nogami method. The accuracy of the method is tested for the Krumlinde-Szymański R(5) model. The results of calculations are compared with those obtained from the standard mean field theory and particle-number projection method, and with exact solutions.

PACS number(s): 21.60.−n, 21.10.Ma, 02.90.+p

I. INTRODUCTION

The mean-field approach to the phenomenon of superconductivity introduced by Bardeen, Cooper, and Schrieffer (BCS) [1] allows for a simple and elegant treatment of pairing correlations in nuclei [2,3]. The main drawback of the BCS method is that its wave function is not an eigenstate of the particle number operator. The accuracy of the BCS approximation is satisfactory if the pairing interaction strength is strong or the number of particles is very large [4,5]. These conditions are not satisfied in nuclei. Indeed, the critical value of the effective pairing strength, G_{crit}, above which the static gap exists, is inversely proportional to the single-particle level density around the Fermi level [3], i.e., it becomes very large around subshell closures.

It was demonstrated by Lipkin [6] that the effect of the nucleon number fluctuation can be suppressed by using a model Hamiltonian $\hat{H} - \lambda_1 \hat{N} - \lambda_2 \hat{N}^2$ instead of the conventional Routhian $\hat{H} - \lambda \hat{N}$, where $\hat{H}$ is the original Hamiltonian (involving pairing interaction) and $\hat{N}$ is the nucleon number operator. The approach by Lipkin was then developed by Nogami and his collaborators [7–11]. The important feature of the Lipkin-Nogami (LN) method is that (i) there always exists a nontrivial (superfluid) solution regardless of the strength of pairing force and (ii) the LN wave function has a similar form to that of the BCS method, thus allowing a simple interpretation of excited states in terms of quasiparticles.

In this respect it seems to be of considerable interest to extend the LN method to the case of rotation, where the short-ranged attractive pairing force plays a significant role. For instance, at low spins the pairing correlations tend to significantly reduce the nuclear moment of inertia as compared to the rigid-body estimate. On the other hand, it was well known that at very high spins many nuclei behave as macroscopic rotors, i.e., their moments of inertia are fairly constant and close to their rigid-body values. More examples illustrating the importance of pairing correlations at high spins can be found in the review in Ref. [12].

In this connection further studies of the Mottelson-Valatin effect [13] (phase transition from superfluid to normal state in rotating nuclei) are of great importance [14,12]. Since the BCS method provides a rather poor description of the pairing phase transition region, one expects that the LN method would be a powerful tool allowing for a better description of pairing correlations without losing the simplicity of the rotating independent quasiparticle picture.

The LN method is recently receiving a fairly large interest both in the model studies [15,16] and in applications [17–20]. However, it has not yet been applied to the case of Hartree-Fock-Bogoliubov (HFB) theory but only in connection with a simple BCS approach. The main objective of this paper is to generalize the LN prescription to the case of HFB. In particular, we concentrate on the influence of the cranking term on pairing correlations, i.e., we consider the HFB theory with broken time-reversal symmetry.

In Sec. II the cranked LN (LNC) equations are derived. The equation for the particle number fluctuation is explicitly written in terms of the single-particle and pair densities. This will be useful when adopting the LN approach to the general HFB treatment. The method is applied in Sec. III to the exactly solvable two-level cranking model with pairing. The exact solutions are compared to those obtained within the standard mean-field approach, particle number projection method, LNC treatment, and

*Permanent address: Institute of Theoretical Physics, Warsaw University, Hoża 69, 00-681 Warsaw, Poland; Institute of Physics, Warsaw University of Technology, Warsaw, Poland.

its particle-number projected version. The conclusions are presented in Sec. IV.

II. THE METHOD

A. Cranked Lipkin-Nogami equations

Let us consider the BCS Hamiltonian which contains a single-particle Hamiltonian, $\hat{H}_{\rm sp}$, and a seniority pairing (monopole, state independent) interaction:

$$\hat{H} = \hat{H}_{\rm sp} + \hat{H}_{\rm pair} = \sum_k e_k a_k^\dagger a_k - G \sum_{k,l>0} a_k^\dagger a_{\bar{k}}^\dagger a_{\bar{l}} a_l,$$

(2.1)

where e_k is the single-particle energy, G is the pairing strength, and $|\bar{k}\rangle = \hat{T}|k\rangle$.

In order to investigate the pairing interaction in rotating system we consider the cranking Hamiltonian (Routhian):

$$\hat{H}^\omega = \hat{H}_{\rm sp} + \hat{H}_{\rm pair} - \omega \hat{j}_x,$$

(2.2)

where $\hat{j}_x$ denotes the component of the total nucleonic angular momentum on the rotational axis (here x axis). This axis is assumed to be fixed in space (only one-dimensional rotation is considered) and the angular velocity of rotation, ω, is supposed to be constant.

In the standard rotating BCS (RBCS) approach the expectation value of the Routhian (2.2), $E^\omega = \langle \hat{H}^\omega \rangle$, is minimized in the product state of independent quasiparticles defined through the Bogolyubov transformation:

$$\alpha_i^\dagger = \sum_l (A_{li} a_l^\dagger + B_{li} a_l),$$

$$\alpha_i = \sum_l (A_{li}^* a_l + B_{li}^* a_l^\dagger),$$

(2.3)

where $\alpha_i^\dagger$ (α_i) is the quasiparticle creation (annihilation) operator. The RBCS wave function represents a mixture of states with different numbers of particles. Consequently, in order to account for the fluctuations, the particle number should be projected before variation. This can be done in a good approximation by means of the LN method outlined below.

Let us assume that the state $|\psi_n\rangle$ is the quasiparticle vacuum, i.e.,

$$\alpha_i |\psi_n\rangle = 0.$$

(2.4)

The index n stands for the average number of particles in the state $|\psi_n\rangle$, determined by means of the particle number equation

$$\langle \psi_n | \hat{N} | \psi_n \rangle = n,$$

(2.5)

where $\hat{N} = \sum_k a_k^\dagger a_k$ is the particle number operator. The state $|\psi_n\rangle$ can be expanded in eigenstates of the particle number operator,

$$|\psi_n\rangle = \sum_{n_0} c_{n,n_0} |\phi_{n_0}\rangle,$$

(2.6)

$$\hat{N} |\phi_{n_0}\rangle = n_0 |\phi_{n_0}\rangle.$$

(2.7)

The total Routhian (2.2) commutes with the particle number operator, $[\hat{H}^\omega, \hat{N}] = 0$. By expanding E^ω in terms of n

$$\langle \phi_n | \hat{H}^\omega | \phi_n \rangle = \lambda(n) = \lambda_0 + \lambda_1 n + \lambda_2 n^2 + \cdots$$

(2.8)

the following relation is obtained:

$$\langle \phi_{n_0} | \hat{H}^\omega | \phi_{n_0} \rangle = \langle \psi_n | \hat{H}^\omega | \psi_n \rangle - \lambda_1 (\langle \psi_n | \hat{N} | \psi_n \rangle - n_0)$$
$$- \lambda_2 (\langle \psi_n | \hat{N}^2 | \psi_n \rangle - n_0^2) - \cdots.$$

(2.9)

The important feature of the above expression is that it yields the expectation value of $\hat{H}^\omega$ in the projected RBCS state, $|\phi_{n_0}\rangle$, in terms of the expectation value of Routhian in the RBCS state, $|\psi_n\rangle$. This implies that, knowing coefficients λ_i, one can minimize the right-hand side of Eq. (2.9) instead of minimizing explicitly the expectation value of $\hat{H}^\omega$ in the projected RBCS state.

So far the considerations are exact. In the next step, however, the expansion (2.9) is truncated by retaining the first m terms; the coefficients $\lambda_1, \lambda_2, ..., \lambda_m$ are then calculated from the following set of linear equations:

$$\langle \psi_n | \hat{K}^\omega \hat{N} | \psi_n \rangle = \langle \psi_n | \hat{K}^\omega | \psi_n \rangle \langle \psi_n | \hat{N} | \psi_n \rangle,$$
$$\langle \psi_n | \hat{K}^\omega \hat{N}^2 | \psi_n \rangle = \langle \psi_n | \hat{K}^\omega | \psi_n \rangle \langle \psi_n | \hat{N}^2 | \psi_n \rangle,$$
$$\vdots$$
$$\langle \psi_n | \hat{K}^\omega \hat{N}^m | \psi_n \rangle = \langle \psi_n | \hat{K}^\omega | \psi_n \rangle \langle \psi_n | \hat{N}^m | \psi_n \rangle,$$

(2.10)

where $\hat{K}^\omega = \hat{H}^\omega - \lambda_1 \hat{N} - \lambda_2 \hat{N}^2 - \cdots - \lambda_m \hat{N}^m$. The $m = 1$ case, together with the constraint (2.5), is equivalent to the standard RBCS method. The case of $m=2$ is discussed below. The generalization to higher orders is straightforward although algebraic manipulations become tedious.

In the LN method the expectation value of $\hat{K}^\omega$ is minimized assuming that coefficients λ_1 and λ_2 are constant (the simultaneous variation of λ's would lead to more complicated equations [5]):

$$\delta \langle \psi_n | \hat{K}^\omega | \psi_n \rangle = 0.$$

(2.11)

The Lagrange multipliers λ and ω are determined by fixing expectation values of the particle number and angular momentum, respectively,

$$\langle \psi_n | \hat{N} | \psi_n \rangle = n,$$

(2.12)

$$\langle \psi_n | \hat{j}_x | \psi_n \rangle = I.$$

(2.13)

It is convenient to express the results through the density matrices ρ and u and the pairing tensor χ, which are defined by means of the transformation matrices A and B:

$$\rho_{kl} = \sum_i B^*_{ki} B_{li},$$

$$u_{kl} = \sum_i A^*_{ki} A_{li} = \delta_{kl} - \rho_{kl}, \qquad (2.14)$$

$$\chi_{kl} = \sum_i A_{li} B^*_{ki}.$$

Expressed in terms of quasiparticles the operator $\hat{K}^\omega$ takes the form

$$\hat{K}^\omega = K^\omega_{00} + \hat{K}^\omega_{11} + \hat{K}^\omega_{20} + \hat{K}^\omega_{22} + \hat{K}^\omega_{31} + \hat{K}^\omega_{40}, \qquad (2.15)$$

where

$$K^\omega_{00} = \sum_{k,l} [e_k \delta_{kl} - \omega(j_x)_{kl}] \rho_{kl} - \frac{\Delta^2}{G} - \frac{1}{2} G \sum_{k,l} \rho_{kl} \rho_{\bar{k}\bar{l}}$$
$$- \lambda_1 n - \lambda_2 n^2 - 2\lambda_2 \sum_{k,l} \rho_{kl} u_{kl}, \qquad (2.16)$$

$$\hat{K}^\omega_{11} = \sum_{i,j} \left\{ \left[\sum_{k,l} [\epsilon_{kl} - \lambda - \omega(j_x)_{kl}](A^*_{ki} A_{lj} - B_{kj} B^*_{li}) \right.\right.$$
$$\left.\left. + \Delta_{kl} A^*_{ki} B_{lj} - \Delta^*_{kl} B^*_{ki} A_{lj} \right] + \lambda_2 \delta_{ij} \right\} \alpha^\dagger_i \alpha_j, \qquad (2.17)$$

$$\hat{K}^\omega_{20} = \sum_{i,j} \left\{ \sum_{k,l} [\epsilon_{kl} - \lambda - \omega(j_x)_{kl}] A^*_{ki} B^*_{lj} \right.$$
$$\left. + \frac{1}{2} \Delta_{kl} A^*_{ki} B^*_{lj} + \frac{1}{2} \Delta^*_{kl} B^*_{li} B^*_{kj} \right\} \alpha^\dagger_i \alpha^\dagger_j + \text{H.c.} \qquad (2.18)$$

The terms $\hat{K}^\omega_{22}$, $\hat{K}^\omega_{31}$, $\hat{K}^\omega_{40}$ represent the residual interaction between quasiparticles and are neglected in this approximation. In the above relations the following quantities are introduced:

$$\epsilon_{kl} = e_k \delta_{kl} - G \text{sgn}(k) \text{sgn}(l) \rho_{\bar{k}\bar{l}} + 4\lambda_2 \rho^*_{kl}, \qquad (2.19)$$

$$\lambda = \lambda_1 + 2\lambda_2(n+1), \qquad (2.20)$$

$$\Delta_{kl} = -\delta_{k\bar{l}} \text{sgn}(k) \Delta = -G \delta_{k\bar{l}} \text{sgn}(k) \sum_{k>0} \chi_{k\bar{k}}. \qquad (2.21)$$

Condition (2.11) leads to the HFB equations:

$$\sum_l \{ (\nu^\omega_{kl} - \lambda \delta_{kl}) A_{li} + \Delta_{kl} B_{li} \} = \mathcal{E}^\omega_i A_{ki},$$
$$\sum_l \{ (\nu^{\omega*}_{kl} - \lambda \delta_{kl}) B_{li} + \Delta^*_{kl} A_{li} \} = -\mathcal{E}^\omega_i B_{ki}, \qquad (2.22)$$

where

$$\nu^\omega_{kl} = \epsilon_{kl} - \omega(j_x)_{kl}, \qquad (2.23)$$

$$\mathcal{E}^\omega_i = E^\omega_i - \lambda_2. \qquad (2.24)$$

The difference between the usual HFB equations and the above ones consists in the appearance of the parameter λ_2 which should be determined self-consistently from Eq. (2.10). It is important to note, that the eigenvalues of the LN+HFB equations (2.22), $\mathcal{E}^\omega_i$, are related to quasiparticle Routhians E^ω_i through relation (2.24). Consequently, special care should be taken when interpreting the results using the standard technique of quasiparticle diagrams of the cranked shell model.

The total LNC energy of the quasiparticle vacuum is given by

$$E_{\text{LNC}} = K^\omega_{00} + \lambda_1 n + \lambda_2 n^2 + \omega I$$
$$= \sum_k e_k \rho_{kk} - \frac{\Delta^2}{G} - \frac{1}{2} G \sum_{k,l} \rho_{kl} \rho_{\bar{k}\bar{l}}$$
$$- 2\lambda_2 \sum_{k,l} \rho_{kl} u_{kl}, \qquad (2.25)$$

where the term proportional to λ_2 represents the nucleon number fluctuation correction.

The presence of self-consistent symmetries very often facilitates the calculations. One such symmetry, important in the context of cranking model and high spins, is the signature symmetry, i.e., the symmetry with respect to the rotation of the system by $180°$ around the x axis. The single-particle states with good signature r are related to the original fermionic basis by the so-called Goodman transformation [21]

$$|K, r = -i\rangle = \frac{1}{\sqrt{2}} \left[-|k\rangle + (-1)^{m_k - \frac{1}{2}} |\bar{k}\rangle \right],$$
$$|\tilde{K}, r = +i\rangle = \frac{1}{\sqrt{2}} \left[(-1)^{m_k - \frac{1}{2}} |k\rangle + |\bar{k}\rangle \right], \qquad (2.26)$$

where m_k is the projection of the single-particle angular momentum on the symmetry axis. Application of transformation (2.26) leads to immediate selection rules for the coefficients of the Bogolyubov transformation,

$$A_{K\bar{L}} = A_{\bar{K}L} = B_{KL} = B_{\bar{K}\bar{L}} = 0, \qquad (2.27)$$

and, consequently, for the matrix elements of the LN+HFB Routhian [21]. In the following it will be assumed that the system is invariant with respect to signature symmetry.

B. Calculation of λ_2

In order to compute λ_2 one can use the set of equations (2.10) which in the case of LNC is reduced to the two relations:

$$\langle \psi_n | \hat{K}^\omega \hat{N} | \psi_n \rangle = \langle \psi_n | \hat{K}^\omega | \psi_n \rangle \langle \psi_n | \hat{N} | \psi_n \rangle,$$
$$\langle \psi_n | \hat{K}^\omega \hat{N}^2 | \psi_n \rangle = \langle \psi_n | \hat{K}^\omega | \psi_n \rangle \langle \psi_n | \hat{N}^2 | \psi_n \rangle. \qquad (2.28)$$

Because of the requirement $\hat{K}^\omega_{20} = 0$, the first equation is satisfied automatically and the second one is simplified to

$$\langle \tilde{0} | \hat{K}^\omega | \tilde{4} \rangle \langle \tilde{4} | \hat{N}^2 | \tilde{0} \rangle = 0, \qquad (2.29)$$

where $|\tilde{0}\rangle$ denotes the quasiparticle vacuum and $|\tilde{4}\rangle\langle\tilde{4}|$ is the projection operator on the four-quasiparticle space. The matrix elements of $\hat{K}^\omega$ and $\hat{N}^2$ that appear in (2.29) are given by

$$\hat{K}^\omega_{40} = \sum_{K,L,P}\left\{\frac{G}{4}B_{KP_1}B_{\tilde{K}P_2}A_{\tilde{L}P_3}A_{LP_4}\right.$$

$$\left.+\lambda_2 B_{KP_1}A_{KP_2}B_{LP_3}A_{LP_4}\right\}\alpha_{P_1}\alpha_{P_2}\alpha_{P_3}\alpha_{P_4}$$

$$+\text{H.c.},\tag{2.30}$$

$$\hat{N}^2_{40} = \sum_{M,N,Q}A^*_{NQ_1}B^*_{NQ_2}A^*_{MQ_3}B^*_{MQ_4}\alpha^\dagger_{Q_1}\alpha^\dagger_{Q_2}\alpha^\dagger_{Q_3}\alpha^\dagger_{Q_4} \cdot$$

$$+\text{H.c.},\tag{2.31}$$

where we have already applied the Goodman transformation to states with well-defined signature. By means of relations (2.30), (2.31), and (2.29) one can now obtain the expression for λ_2:

$$\lambda_2 = \frac{G}{4}\frac{\sum_{K,L>0}\{\chi^*_{K\tilde{L}}(\rho^*_{\tilde{K}\tilde{L}}+\rho_{KL})\}\sum_{K,L>0}\{\chi_{K\tilde{L}}(u_{\tilde{K}\tilde{L}}+u^*_{KL})\}-2\sum_{K,L}(\chi\chi^\dagger)_{LK}(\chi\chi^\dagger)_{\tilde{L}\tilde{K}}}{\left[\sum_K(\chi\chi^\dagger)_{KK}\right]^2-2\sum_K(\chi\chi^\dagger\chi\chi^\dagger)_{KK}}.\tag{2.32}$$

It is easy to show that for $\omega = 0$ the above relation reduces to the well-known result (see Ref. [11]):

$$\lambda_2 = \frac{G}{4}\frac{\sum_{k>0}(u_kv^3_k)\sum_{k>0}(u^3_kv_k)-\sum_{k>0}(u_kv_k)^4}{\left(\sum_{k>0}u^2_kv^2_k\right)^2-\sum_{k>0}(u_kv_k)^4}.\tag{2.33}$$

Relation (2.32) together with Eqs. (2.22) completes the derivation of the LNC equations.

III. RESULTS FOR THE R(5) MODEL

In order to examine the accuracy of the LNC approximation we consider the two-level Krumlinde-Szymański R(5) model (see [22–24,14,25]). The Hilbert space of this model consists of Ω $j=\frac{3}{2}$ multiplets. As shown in Fig. 1, the single-particle levels are split by the deformation of the average nuclear potential. The single-particle splitting is $2e$, i.e., the energy of the upper levels (labeled as $|1\rangle=|m = 3/2\rangle$ and $|\tilde{1}\rangle=T|1\rangle$) is $+e$ and that of the lower levels (labeled as $|2\rangle=|m = 1/2\rangle$ and $|\tilde{2}\rangle=T|2\rangle$) is $-e$. We begin our analysis by considering the half-filled (symmetric) system, i.e., the number of particles is equal to $n=2\Omega$. In the particular version of the two-level model considered in this paper the Coriolis coupling between
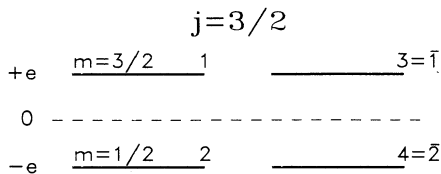
$$j=3/2$$

FIG. 1. Energy levels for the R(5) model. The above pattern is repeated Ω times.

the lower levels is neglected, i.e., $(j_x)_{2\tilde{2}} = 0$. As discussed in Ref. [25], this leads to the absence of signature splitting. In our paper we concentrate on the influence of the time-odd components of the wave function on the LN solution rather then on the comparison with the actual data where the exact treatment of the Coriolis coupling is important. The two-body pairing interaction is assumed to be of the monopole type. The main advantage of this simple model is that it can be solved exactly using the Lie algebra associated with the symmetry group R(5) [23].

In the standard notation of representing HFB equations in doubled dimensions [5], the single-particle field ν has the form of a 4×4 matrix:

$$\hat{\nu}^\omega = \begin{bmatrix} \nu^\omega_u & 0 \\ 0 & \nu^\omega_l \end{bmatrix},\tag{3.1}$$

where

$$\nu^\omega_u = \begin{bmatrix} -e - G\rho_{\tilde{1}\tilde{1}} + 4\lambda_2\rho^*_{11}, & -\omega - G\rho_{\tilde{1}\tilde{2}} + 4\lambda_2\rho^*_{12} \\ -\omega - G\rho_{\tilde{2}\tilde{1}} + 4\lambda_2\rho^*_{21}, & e - G\rho_{\tilde{2}\tilde{2}} + 4\lambda_2\rho^*_{22} \end{bmatrix},\tag{3.2}$$

$$\nu^\omega_l = \begin{bmatrix} -e - G\rho_{11} + 4\lambda_2\rho^*_{\tilde{1}\tilde{1}}, & \omega - G\rho_{12} + 4\lambda_2\rho^*_{\tilde{1}\tilde{2}} \\ \omega - G\rho_{21} + 4\lambda_2\rho^*_{\tilde{2}\tilde{1}}, & e - G\rho_{22} + 4\lambda_2\rho^*_{\tilde{2}\tilde{2}} \end{bmatrix}.\tag{3.3}$$

In the above relation it was assumed that [14,25]

$$(j_x)_{21} = (j_x)_{12} = -(j_x)_{\tilde{2}\tilde{1}} = -(j_x)_{\tilde{1}\tilde{2}} = 1.\tag{3.4}$$

Similarly, the pairing field is given by

$$\hat{\Delta} = -G\Omega(\chi_{1\tilde{1}} + \chi_{2\tilde{2}})\begin{bmatrix} 0 & 0 & 1 & 0 \\ 0 & 0 & 0 & 1 \\ -1 & 0 & 0 & 0 \\ 0 & -1 & 0 & 0 \end{bmatrix}.\tag{3.5}$$

The LNC equations are solved iteratively with respect to the density matrix and pairing tensor. The initial val-

ues can be taken from the standard RBCS equations. Then the coefficient λ_2 is found and the matrices A and B are computed from Eq. (2.22). This gives a new approximation for the density matrix and pairing tensor. One should choose properly λ (the chemical potential) at every iteration step to satisfy the relation $n=\mathrm{Tr}(\rho)$. The above procedure is continued until the convergence is achieved. For more complicated Hamiltonians it is suggested to use the so-called gradient method (see Refs. [26–28]).

Having found the Bogolyubov transformation matrices A and B, one can calculate ρ and u, Eq. (2.14), and then the total energy,

$$E_{\mathrm{tot}} = e\Omega(\rho_{11} + \rho_{\bar{1}\bar{1}} - \rho_{22} - \rho_{\bar{2}\bar{2}})$$
$$- \frac{\Delta^2}{G} - \frac{1}{2}G\Omega\sum_{k,l>0}(\rho_{kl}\rho_{\bar{k}\bar{l}}) - 2\lambda_2\Omega\sum_{k,l>0}(\rho_{kl}u_{kl}),$$
$$(3.6)$$

the pairing energy,

$$E_{\mathrm{pair}} = E_{\mathrm{tot}} - E_{\mathrm{unpair}} = E_{\mathrm{tot}} + 2\Omega e\sqrt{1 - \left(\frac{I}{2\Omega}\right)^2}$$
$$+ G\Omega\left[1 - \left(\frac{I}{2\Omega}\right)^2\right], \quad (3.7)$$

the pairing potential (energy gap),

$$\Delta = G\Omega(\chi_{1\bar{1}} + \chi_{2\bar{2}}), \qquad (3.8)$$

the total angular momentum,

$$I = \mathrm{Tr}(j_x\rho) = 2\Omega(\rho_{12} - \rho_{\bar{1}\bar{2}}). \qquad (3.9)$$

In the light of the recent results [16], it is advantageous to carry out the particle number projection after Lipkin and Nogami (LNC+PNP). This can easily be done by following the formalism of Ref. [14]. The particle-number projected energy and angular momentum are given by

$$E_{\mathrm{tot}}^N = E_{\mathrm{sp}}^N + E_{\mathrm{p1}}^N + E_{\mathrm{p2}}^N, \qquad (3.10)$$

$$I_x^N = 4\Omega\frac{\rho_{12}}{\rho_{(+)} - \rho_{(-)}}\frac{P_{\Omega-1}(\xi)}{P_\Omega(\xi)}, \qquad (3.11)$$

where

$$E_{\mathrm{sp}}^N = -2\Omega e\frac{k}{\rho_{(+)} - \rho_{(-)}}\frac{P_{\Omega-1}(\xi)}{P_\Omega(\xi)} \qquad (3.12)$$

is the single-particle energy, and

$$E_{\mathrm{p1}}^N = -2G\Omega^2\frac{k^2\rho_{(+)}\rho_{(-)}}{[\rho_{(+)} - \rho_{(-)}]^4}\left\{\frac{2\rho_{(+)}\rho_{(-)}}{\Omega - 1}\frac{P'_{\Omega-1}(\xi)}{P_\Omega(\xi)} + [\rho_{(+)} - \rho_{(-)}]\frac{P_{\Omega-1}(\xi)}{P_\Omega(\xi)}\right\} \qquad (3.13)$$

and

$$E_{\mathrm{p2}}^N = -G\Omega\frac{1}{[\rho_{(+)} - \rho_{(-)}]^2}\left\{k^2\left[1 - \frac{4\rho_{(+)}^2\rho_{(-)}^2}{(\Omega - 1)[\rho_{(+)} - \rho_{(-)}]^2}\frac{P'_{\Omega-1}(\xi)}{P_\Omega(\xi)}\right] + 4\rho_{12}^2\left[1 - \xi\frac{P_{\Omega-1}(\xi)}{P_\Omega(\xi)}\right]\right\} \qquad (3.14)$$

are two contributions to the pairing energy (cf. Eqs. (A7) and (A8) of Ref. [14]), and

$$k = \rho_{22} - \rho_{11}, \qquad (3.15)$$

$$\rho_{(\pm)} = \frac{1}{2}\left(1 \pm \sqrt{k^2 + 4\rho_{12}^2}\right), \qquad (3.16)$$

$$\xi = \frac{\rho_{(+)}^2 + \rho_{(-)}^2}{\rho_{(+)} - \rho_{(-)}}. \qquad (3.17)$$

In the above equations $P_n(x)$ is the Legendre polynomial of the nth order. It is easy to see, that in the limit of very weak pairing [$\xi \to 1$, $P_n(1)=1$] the total pairing energy given by Eqs. (3.13) and (3.14) becomes equal to E_{unpair}. On the other hand, if pairing is very strong [$\xi \to \infty$, $P_{n-1}/P_n \to n/(2n - 1)\xi^{-1}$, $P'_{n-1}/P_n \to n(n - 1)/(2n - 1)\xi^{-2}$], the pairing energy approaches the limit of the seniority model, $-G\Omega(\Omega + 1)$.

We have performed calculations within the symmetric variant of the R(5) model for $e=1$, $\Omega=20$ (i.e., the half-filled symmetric system with $n=40$ particles), and for

three values of the pairing strength, $G=0.015$, $G=0.065$, and $G=0.1$ [29]. Without rotation, the mean-field (BCS) solution undergoes a transition to the paired regime at the critical strength $G=2e/(2\Omega - 1)\simeq0.051$. Therefore, the intermediate value of $G=0.065$ corresponds to the phase transition region, and allows us to study the destructive role of rotation on pairing correlations, while the other two values of G represent the weak and strong pairing limits, respectively.

The results of the BCS method are in Figs. 2–5 denoted by the solid triangles and solid circles for RBCS and RBCS+PNP (RFBCS), respectively. The latter results are obtained by the variation after projecting the good particle number component of the RBCS state. The results based on the LNC method are denoted by open symbols. The open triangles and open circles represent the LNC and LNC+PNP (exact particle number projection of LNC solutions) results, respectively. The exact results are denoted by the waterwheel symbols.

Calculations have been performed for ω ranging from 0 to 1.2 [29]. For each ω, the energy and angular momentum have been determined from Eqs. (3.6) and (3.9), or Eqs. (3.10) and (3.11), and the pairing energies have been

computed by means of Eq. (3.7). In this way, the plots of pairing energy versus angular momentum have been constructed and are shown in Fig. 2.

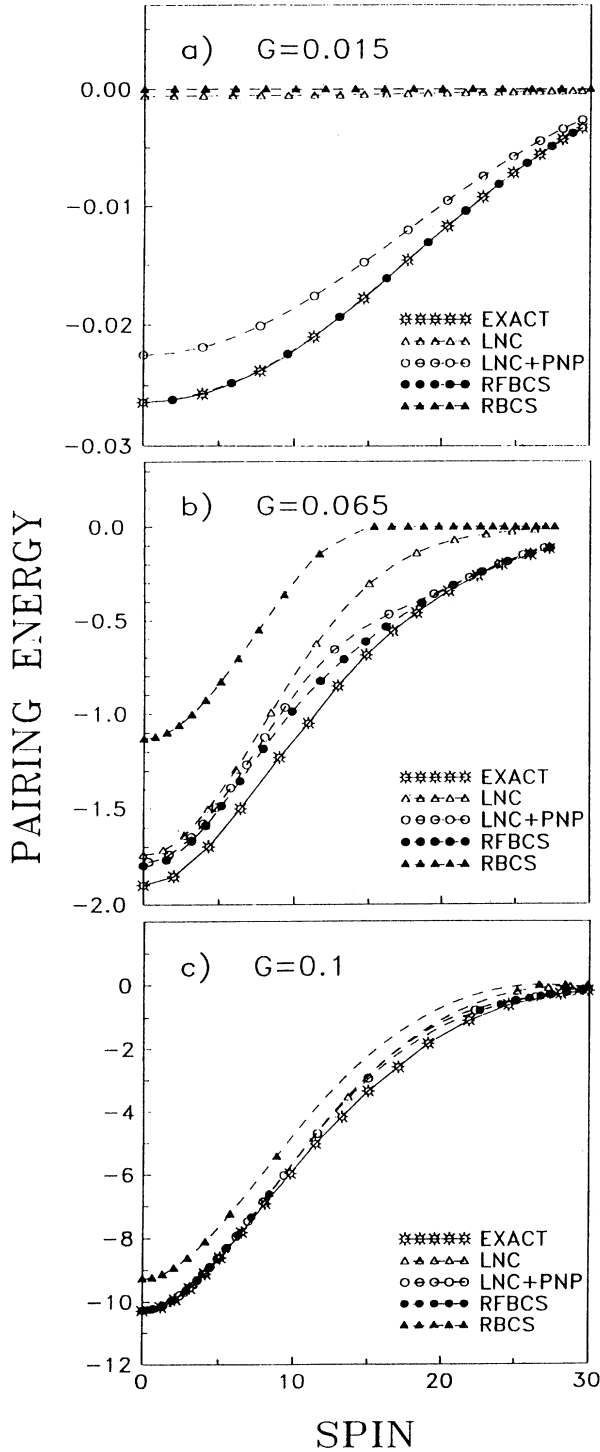For the weak pairing strength, Fig. 2(a), the RBCS

method gives only the unpaired solution for all spin values [25]. Although the solutions of the LNC method contain some pairing correlations, the approximate formula for the energy with the corrective λ_2 term, Eq. (3.6), gives the pairing energy much too small. On the other hand, when the LNC solutions are projected on the good particle number one obtains a fair qualitative agreement with the exact results (the maximum relative difference is of the order of 20%). This illustrates the fact that the LNC wave function describes resonable well the pairing correlations in a weak-pairing limit even if the average value of the auxiliary Hamiltonian $\hat{K}^\omega$ is not a very good approximation to the exact energy of the system.

As seen in Fig. 2(a), the RFBCS results provide an excellent approximation to the exact values. This indicates, that there is still some room for improvements of the LNC+PNP method. From Ref. [16] it follows that the difficulties of the LN method in describing the half-filled ($n=2\Omega$) system in the weak-pairing limit stem from the fact that its exact ground-state energy cannot be approximated by a second-order expansion in n centered at $n_0=2\Omega$. However, the parabolic expansion works very well for the ground-state energies of *asymmetric* systems with $n\neq 2\Omega$. Based on this result, a useful two-step procedure is suggested. Firstly, the LN or LNC equations are solved for the system with $n_0=2\Omega \pm 2$. In the second step, the $n=2\Omega$ component is projected out from the resulting LNC wave function. Such a hybrid method relies on *extrapolating* the $n=2\Omega$ solution from *either* those for $n<2\Omega$ *or* those for $n>2\Omega$, instead of *interpolating* between solutions for $n<2\Omega$ *and* those for $n>2\Omega$. Results of LN+PNP calculations for $n_0=2\Omega+2=42$ are presented in Fig. 3 and agree remarkably well with those using the RFBCS method and with the exact values.

The weak-pairing regime is realized in nuclei around shell or subshell closures where $e\gg G\Omega$. Therefore, the hybrid method described above can be useful for study-

FIG. 2. Pairing energy versus angular momentum for three values of pairing strength, (a) $G=0.015$, (b) $G=0.065$, and (c) $G=0.1$.
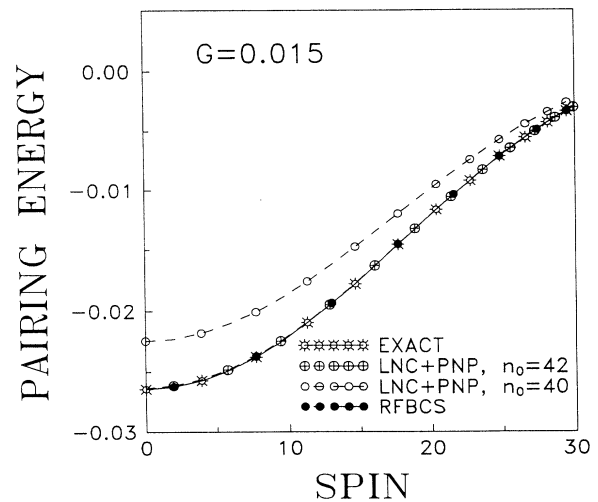

FIG. 3. Pairing energy versus angular momentum for the weak pairing strength, $G=0.015$. The LNC+PNP results calculated for $n=2\Omega=40$ from the $n_0=42$ solutions are also shown.

ing properties of, e.g., spherical magic nuclei at low spin or superdeformed magic nuclei ([152]Dy or [192]Hg) at high spin.

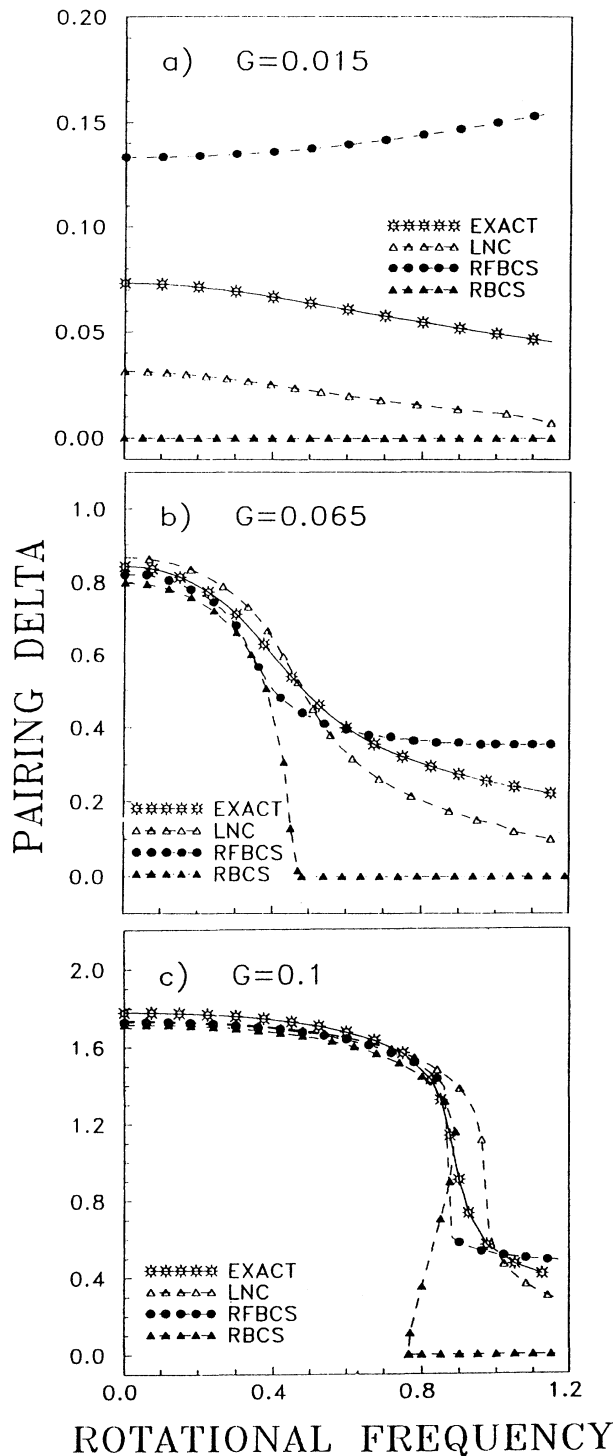For the intermediate pairing strength, Fig. 2(b), the RBCS method yields the unpaired solution above a cer-

tain critical angular momentum. Such a sharp transition is not present in the exact results. Although the low-spin LNC results are in much better agreement with the exact solutions than those of the RBCS method, this method yields too small a pairing energy at higher spins. Not surprizing, the pairing energies of the PNP+LNC method agree quite well with those obtained by means of the RFBCS treatment. The latter ones describe fairly well the exact values, while the remaining small difference, which cannot be accounted for by using the BCS-type wave function, illustrates the presence of large correlations (due to the quasiparticle interaction) at the phase transition region.

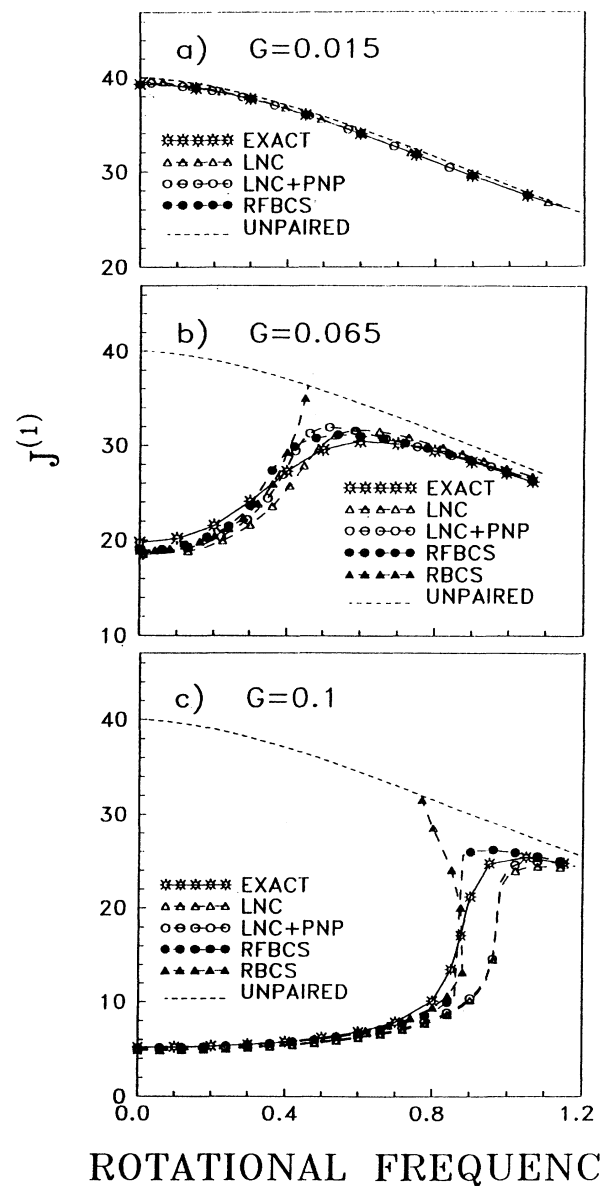For the strong pairing limit, Fig. 2(c), the RBCS

FIG. 4. Pairing Δ versus rotational frequency ω_I for three values of pairing strength, (a) $G=0.015$, (b) $G=0.065$, and (c) $G=0.1$.

FIG. 5. Kinematical moment of inertia versus rotational frequency ω_I for three values of pairing strength, (a) $G=0.015$, (b) $G=0.065$, and (c) $G=0.1$.

method is the only one which fails to describe exact results. All other methods give very good agreement at low and high angular momenta and leave a gap of missing solutions around $I=18$, i.e., in the region where the adiabatic cranking approximation breaks down (the solutions in the phase transition region correspond to the maximum of the total Routhian rather than to the minimum [14]). Interestingly, the region of instability is very large for the RFBCS method, where it extends down to $I=10$, while the LNC method is able to follow solutions up to $I=16$. The particle number projection does not lead to a significant improvement here.

Figure 4 shows the pairing delta Δ_{BCS} as a function of ω. This quantity characterizes the BCS states used in RBCS, LNC, and RFBCS methods and defines the BCS occupation probabilities (for the LN occupation probabilities, see, e.g., Ref. [19]). In fact, in the methods employing the concept of PNP, Δ_{BCS} is not related to any particular observable; it should not be understood as the energy gap, but rather as a variational parameter (see Ref. [14]). Figure 4 shows Δ_{BCS} together with $\Delta_{\text{exact}} \equiv \sqrt{-G\langle \hat{H}_{\text{pair}} \rangle}$ where the average value is calculated with respect to the exact ground-state wave function. By definition, Δ_{exact} is a direct measure of pairing correlations and it should reflect Δ_{BCS} in the limit of large pairing. Note that the Δ_{BCS} parameter for LNC+PNP is the same as for LNC, and, therefore, is not shown in Fig. 4. It is seen in Fig. 4(a) that in the weak pairing limit the two quantities Δ_{exact} and Δ_{BCS} differ very much even if the RFBCS pairing energy is rather close to exact values, Fig. 2. In the intermediate and strong pairing limits the Δ_{BCS} parameter of RBCS goes to zero at the critical angular momentum, which illustrates the Mottelson-Valatin phase transition. The exact results do not show such a sharp transition, and the Δ_{BCS} parameters of the LNC and RFBCS method qualitatively reproduce the exact values.

The angular momentum alignment is illustrated in Fig. 5 where the kinematical moment of inertia,

$$\mathcal{J}^{(1)} = \frac{I}{\omega_I}, \qquad (3.18)$$

is shown as a function of rotational frequency ω_I. At this point it should be stressed that the rotational frequency, ω_I, obtained from the canonical relation

$$\omega_I = \frac{dE}{dI} \qquad (3.19)$$

is equivalent to the cranking-model frequency ω only for the exact eigenstates of a model cranking Hamiltonian. Consequently, the relation

$$\omega = \omega_I \qquad (3.20)$$

holds exactly for the exact solutions of the R(5) model, and also for the RBCS variant (the solution is an eigenstate of the independent-quasiparticle Hamiltonian). On the other hand, the relation (3.20) does not hold for the approaches based on the PNP treatment, since the resulting states are determined from the *restricted* variational

principle. Consequently, the rotational frequency in Fig. 5 is determined using Eq. (3.19). The moment of inertia, Eq. (3.18), illustrates the Mottelson-Valatin phase transition. It can be seen that for all pairing strengths the LNC
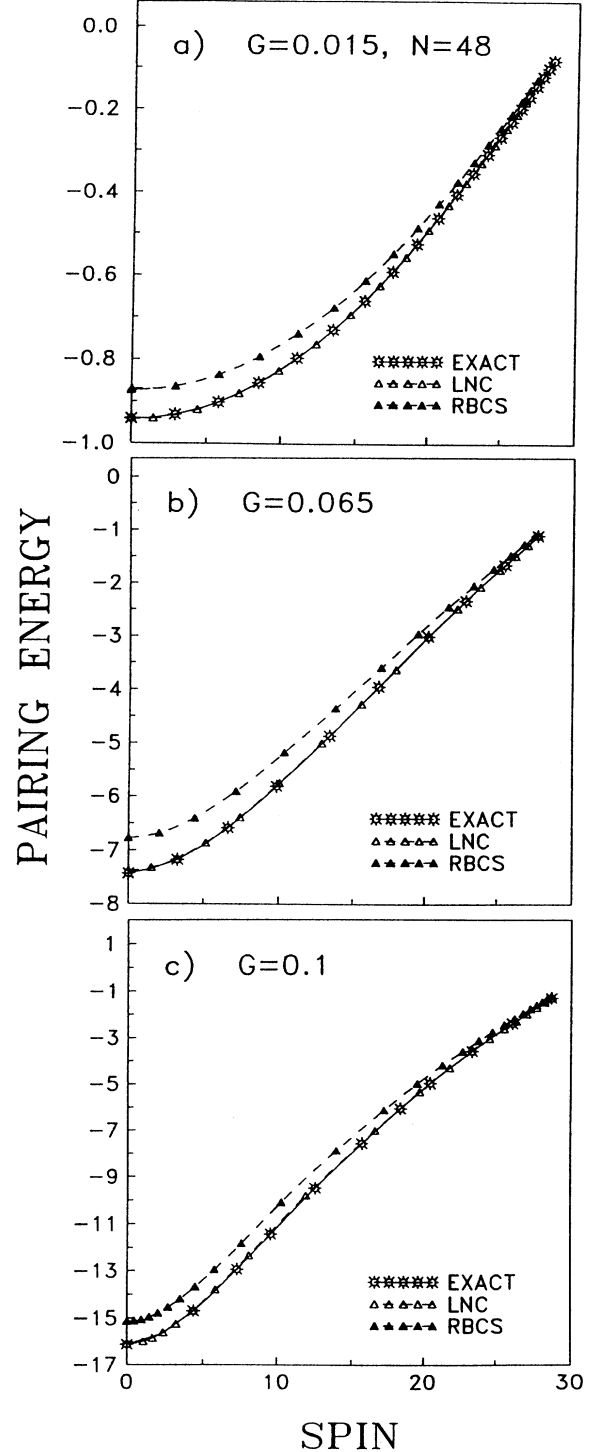

FIG. 6. Pairing energy versus angular momentum for the asymmetric variant of the R(5) model with $n=48$ and for three values of pairing strength, (a) $G=0.015$, (b) $G=0.065$, and (c) $G=0.1$. Only the exact, RBCS and LNC results are displayed.

method correctly describes this transition, both with and without the subsequent particle number projection.

We have also performed calculations for the asymmetric system, $n \neq 2\Omega$. Here, the static RBCS solution is always present, independently of the value of the pairing strength [25], and the results and conclusions are very similar to those for the symmetric system, $n=2\Omega$, in the strong pairing limit. The results for the $n=48$ system are shown in Fig. 6. It is seen that the LNC method provides an excellent approximation to the pairing energy, even without a subsequent particle number projection.

IV. CONCLUSIONS

We have studied the pairing correlations in rotating nuclei using the cranked Lipkin-Nogami LNC method which is based on employing the auxiliary Hamiltonian $\hat{K}^\omega = \hat{H} - \lambda_1 \hat{N} - \lambda_2 \hat{N}^2 - \omega \hat{j}_x$, where the parameters λ_1 and λ_2 are chosen so that the influence of the nucleon number fluctuation is strongly reduced. One should emphasize the simplicity of the LNC approximation, especially when compared with more sophisticated projection methods. In practice, the LNC method is a simple extension of the usual RBCS treatment.

Good accuracy was obtained for the ground-state energy, particularly in the case of strong pairing interaction. It means that the method suppresses correctly the "dan-gerous" (particle-number violating) part of the quasiparticle interaction. The weakness of the LNC method in the weak pairing limit can be overcome by performing the projection *after* variation. Therefore, the LNC+PNP approach can provide us with a fair description of rotating nuclei near shell and subshell closures.

Another welcome feature of the LNC method is that it provides us with a very good description of the pairing phase transition region, regardless of the strength of pairing interaction. Note that using the LNC method one can obtain nontrivial solutions even for very fast rotation where the RBCS method breaks down.

ACKNOWLEDGMENTS

[1] J. Bardeen, L.N. Cooper, and J.R. Schrieffer, Phys. Rev. **108**, 1175 (1957).

[2] A. Bohr, B.R. Mottelson, and D. Pines, Phys. Rev. **110**, 936 (1958).

[3] S.T. Belyaev, Mat. Fys. Medd. Dan. Vid. Selsk. **31** (No. 11) (1959).

[4] A.M. Lane, *Nuclear Theory* (Benjamin, New York, 1964).

[5] P. Ring and P. Schuck, *The Nuclear Many Body Problem* (Springer, New York, 1980).

[6] H.J. Lipkin, Ann. Phys. (N.Y.) **9**, 272 (1960).

[7] Y. Nogami, Phys. Rev. **313**, B134 (1964).

[8] Y. Nogami and I.J. Zucker, Nucl. Phys. **60**, 203 (1964).

[9] Y. Nogami, Phys. Lett. **15**, 4 (1965)

[10] J.F. Goodfellow and Y. Nogami, Can. J. Phys. **44**, 1321 (1966).

[11] H.C. Pradhan, Y. Nogami, and J. Law, Nucl. Phys. **A201**, 357 (1973).

[12] Y.R. Shimizu, J.D. Garrett, R.A. Broglia, M. Gallardo, and E. Vigezzi, Rev. Mod. Phys. **61**, 131 (1989).

[13] B.R. Mottelson and J.G. Valatin, Phys. Rev. Lett. **5**, 511 (1960).

[14] W. Nazarewicz, J. Dudek, and Z. Szymański, Nucl. Phys. **A436**, 139 (1985).

[15] D.C. Zheng, D.W.L. Sprung, and H. Flocard, Phys. Rev. C **46**, 1355 (1992).

[16] J. Dobaczewski and W. Nazarewicz, Phys. Rev. C **47**, 2418 (1993)

[17] W. Nazarewicz, M.A. Riley, and J.D. Garrett, Nucl. Phys. **A512**, 61 (1990).

[18] P. Möller and J.R. Nix, Nucl. Phys. **A536**, 20 (1992).

[19] L. Bennour, P.-H. Heenen, P. Bonche, J. Dobaczewski, and H. Flocard, Phys. Rev. C **40**, 2834 (1989).

[20] P.-H. Heenen, P. Bonche, J. Dobaczewski, and H. Flocard, Nucl. Phys. A (to be published).

[21] A.L. Goodman, Nucl. Phys. **A230**, 466 (1974).

[22] J. Krumlinde and Z. Szymański, Phys. Lett. **36B**, 157 (1971).

[23] J. Krumlinde and Z. Szymański, Ann. Phys. (N.Y.) **79**, 201 (1973).

[24] S.Y. Chu, E.R. Marshalek, P. Ring, J. Krumlinde, and J.O. Rasmussen, Phys. Rev. C **12**, 1017 (1975).

[25] D.R. Bés, R.A. Broglia, J. Dudek, W. Nazarewicz, and Z. Szymański, Ann. Phys. (N.Y.) **182**, 237 (1988).

[26] H.J. Mang, B. Samadi, and P. Ring, Z. Phys. A **279**, 325 (1976).

[27] J.L. Egido and P. Ring, Nucl. Phys. **A383**, 189 (1982).

[28] J.L. Egido and P. Ring, Nucl. Phys. **A388**, 19 (1982).

[29] All energies are supposed to be expressed in the same units, say MeVS, and the units are not shown explicitly.